Translational Oncology
www.transonc.com

Volume 8 Number 4 August 2015 pp. 295–307 295

Cyclin-Dependent Kinase 5 (CDK5) Controls Melanoma Cell Motility, Invasiveness, and Metastatic Spread—Identification of a Promising Novel therapeutic target[1]

Savita Bisht*, Jens Nolting*, Ute Schütte*, Jens Haarmann*, Prashi Jain†, Dhruv Shah†, Peter Brossart*, Patrick Flaherty† and Georg Feldmann*

*Department of Internal Medicine 3, Center of Integrated Oncology (CIO) Cologne-Bonn, University Hospital of Bonn, Germany; †Mylan School of Pharmacy, Medicinal Chemistry, Duquesne University, Pittsburgh, PA

Abstract

Despite considerable progress in recent years, the overall prognosis of metastatic malignant melanoma remains poor, and curative therapeutic options are lacking. Therefore, better understanding of molecular mechanisms underlying melanoma progression and metastasis, as well as identification of novel therapeutic targets that allow inhibition of metastatic spread, are urgently required. The current study provides evidence for aberrant cyclin-dependent kinase 5 (CDK5) activation in primary and metastatic melanoma lesions by overexpression of its activator protein CDK5R1/p35. Moreover, using melanoma *in vitro* model systems, shRNA-mediated inducible knockdown of CDK5 was found to cause marked inhibition of cell motility, invasiveness, and anchorage-independent growth, while at the same time net cell growth was not affected. *In vivo*, CDK5 knockdown inhibited growth of orthotopic xenografts as well as formation of lung and liver colonies in xenogenic injection models mimicking systemic metastases. Inhibition of lung metastasis was further validated in a syngenic murine melanoma model. CDK5 knockdown was accompanied by dephosphorylation and overexpression of caldesmon, and concomitant caldesmon knockdown rescued cell motility and proinvasive phenotype. Finally, it was found that pharmacological inhibition of CDK5 activity by means of roscovitine as well as by a novel small molecule CDK5-inhibitor, *N*-(5-isopropylthiazol-2-yl)-3-phenylpropanamide, similarly caused marked inhibition of invasion/migration, colony formation, and anchorage-independent growth of melanoma cells. Thus, experimental data presented here provide strong evidence for a crucial role of aberrantly activated CDK5 in melanoma progression and metastasis and establish CDK5 as promising target for therapeutic intervention.

Translational Oncology (2015) 8, 295–307

Introduction

Malignant melanoma is the seventh most common newly diagnosed cancer in women and the fifth most common in men in the Western world. Incidence rates for melanoma are increasing, as opposed to stable or declining trends observed in most other cancer types [1]. Over the past years, considerable progress has been made in the treatment of advanced, metastatic disease stages with the advent of novel immunotherapeutic strategies and targeted therapies [2–4]. Nevertheless, metastatic melanoma still carries an extremely poor overall prognosis, and curative strategies are still lacking [5]. Despite the prominent role metastasis plays for melanoma patients from a clinical point of view, all attempts to therapeutically prevent metastatic spread have been futile so far. Therefore, better understanding of the pathophysiological mechanisms underlying melanoma progression and metastasis on a molecular level and identification of potential druggable targets to prevent these processes are urgently required.

Address all correspondence to: Georg Feldmann, MD, Department of Internal Medicine 3, Center of Integrated Oncology (CIO) Cologne-Bonn, University Hospital of Bonn, Sigmund-Freud-Str. 25, D-53127 Bonn, Germany.
E-mail: georg.feldmann@uni-bonn.de

[1] The authors confirm that there is no conflict of interests that might impair the impartiality of this scientific work.

Received 17 May 2015; Revised 16 June 2015; Accepted 23 June 2015

1936-5233/15
http://dx.doi.org/10.1016/j.tranon.2015.06.002

Cyclin-dependent kinase 5 (CDK5) has initially been described as crucially involved in regulating neuronal migration during brain development [6]. Increasing evidence is being accumulated only in recent years suggesting additional functions of CDK5 outside the nervous system [7,8]. Of interest, studies from our own group as well as by others suggest that similarities exist between early neuronal migration during embryogenesis and metastatic spread of malignant tumors. It was hypothesized that CDK5 modulates oncogenic signaling pathways involved in conferring a prometastatic, invasive phenotype and might be a suitable therapeutic target that could allow to specifically prevent metastatic tumor spread in certain entities [9–11]. This current study examines the role of CDK5 and possible effectors involved in progression and metastatic spread of malignant melanoma using primary tissue samples as well as relevant functional *in vitro* and *in vivo* model systems.

Materials and Methods

Cell Culture

Human melanoma cell lines A375, SKmel28, FM8, Mel1479, and DO8 and murine cell lines B16F10 and 1274mel were cultured in RPMI1640 media (PAA Laboratories, Pasching, Austria) supplemented with 10% FBS, 1 × penicillin/streptomycin (PAA Laboratories), and 5 μg/mL plasmocin (InvivoGen, San Diego, CA). 293 FT cells were maintained in DMEM containing 10% FBS, 0.1 mM nonessential amino acids, 1 mM sodium pyruvate, and 1 × penicillin/streptomycin (all PAA Laboratories) as well as 5 μg/mL plasmocin (InvivoGen). All the cell lines were grown in a humidified atmosphere at 37°C in the presence of 5% CO_2 and were routinely tested for mycoplasma infection using a polymerase chain reaction(PCR)–based assay as described elsewhere [12].

Lentivirus Production and Generation of Stable Cell Lines

To generate stable cell lines, a target set of shRNA sequences directed against human CDK5 in an inducible pTRIPZ-Tet-On expression vector system (Thermo Scientific, Waltham, MA) was used. Clones that showed more than 90% knockdown efficiency in the presence of doxycycline were used for further experiments and designated as CDK5-shRNA#F10 (Clone ID-V3THS 390940) and CDK5-shRNA#B7 (Clone ID-V3THS 390939). For murine cell lines, a target set of shRNA sequences against murine CDK5 in pGIPZ expression vector system was also obtained from Thermo Scientific, and the clone showing efficient knockdown was used and designated as murine CDK5shRNA#1 (Clone ID-V2LMM 2408). Empty vectors, pTRIPZ and pGIPZ, respectively, containing no shRNA inserts were used as negative controls.

For lentivirus production, 293FT-packaging cells were co-transfected with pCMV-VSVg, pCMV-dR8.74, and the respective pTRIPZ and pGIPZ plasmids using calcium phosphate method as previously mentioned [13]. Supernatant containing lentivirus was harvested after 48 and 72 hours and used to transduce human or murine melanoma cell lines. Resistant clones were selected and maintained in the presence of puromycin (2 μg/ml) throughout all *in vitro* experiments.

Cell Viability (3-(4,5-Dimethyl-2-yl)-5-(3-Carboxymethoxyphenyl)-2-(4-Sulfophenyl)-2H-Tetrazolium) Assays

Cell viability was determined using 3-(4,5-dimethyl-2-yl)-5-(3-carboxymethoxyphenyl)-2-(4-sulfophenyl)-2H-tetrazolium (MTS) assay as previously described [14]. Briefly, 2000 cells per well were plated in full growth media with or without doxycycline (2 μg/ml) for 0, 24, 48, and 72 hours, respectively. At each time point, the assay was terminated and relative cell growth was determined using the CellTiter 96 reagent (Promega, Madison, WI), as recommended in the manufacturer's protocol. All experiments were set up in triplicates, and the results were normalized to the mean cell viability at 0 hours.

Soft Agar Assays

Soft agar assays were set up in six-well plates as described previously [15]. In brief, a base agar layer was formed by mixing 2 ml of media and 1% agarose on top of which a second layer of 2 ml of media containing 0.7% agarose and 10,000 cells was poured and allowed to solidify. Finally, 2 ml of media was added on top of the agarose layers, and the plates were incubated at 37°C for 4 weeks. When colonies became visible, cells were stained with 0.005% (w/v) crystal violet solution (Sigma Aldrich, Steinheim, Germany) and visualized by trans-UV illumination (BioRad, Hercules, CA). Colonies were counted, and colony counts were normalized to the mean colony count of the respective uninduced controls. All assays were set up in triplicates.

Cell Motility Assays

To test the effect of CDK5 knockdown on motility of melanoma cells, wound-healing assays were performed using fibronectin-coated plates. Stably transfected cells were grown to near confluency in 24-well plates coated with fibronectin (25 μg/well). A scratch was made using a pipette tip, cell debris was removed by washing twice with PBS, and further media was added to cells. Light microscopic images were taken at 0 and 22 hours, respectively.

Invasion Assays

To determine the invasive potential of cells, Boyden chambers with 8 μm pore size filters coated with Matrigel (50 μg per chamber; BD Biosciences, San Jose, CA) were used. A total of 30,000 cells/well were placed in the upper chamber and incubated at 37°C for 72 hours, at which time cells that had invaded to the lower side of the filter were fixed in 70% ethanol and stained with hematoxylin and eosin (H&E). Membranes were then mounted onto glass slides and examined microscopically. Cells were counted in five randomly selected microscopic fields, and means and standard deviations were calculated.

Western Blot

Cells were lysed using radioimmunoprecipitation assay buffer (1% Igepal CA630, 0.5% sodium deoxycholate, 0.1% SDS, 2 mM EDTA) supplemented with protease and phosphatase inhibitor cocktails (Sigma Aldrich). Fifty micrograms of total protein was separated using 4% to 12% Nupage bis-tris gels (Life Technologies, Darmstadt, Germany) and transferred onto PVDF membranes (Millipore, Billerica, MA). The blots were blocked using either 5% (w/v) BSA or 5% (w/v) milk in TBST for 1 hour and then later probed using primary antibodies against CDK5R1p35, CDK5, caldesmon, GAPDH (all used at a dilution of 1:1000; Cell Signaling, Danvers, MA) or phospho-caldesmon (Tyr27) (1:500; Santa Cruz Biotechnology, Dallas, TX) as well as HRP-coupled secondary antibodies directed against rabbit or mouse IgG, respectively (1:2000, Cell Signaling). Detection was performed as previously described [16].

RNA Extraction and Reverse Transcription Quantitative PCR

For quantitative real-time reverse transcription (RT)–PCR analysis, cells were lysed and total RNA was extracted using RNeasy mini

kits including on-column DNA digestion (Qiagen, Hilden, Germany). RNA was reverse transcribed using random primers and the High Capacity cDNA Reverse Transcription Kit (Life Technologies) according to the manufacturer's specifications. Real-time quantitative PCR for human CDK5 and caldesmon was performed using the SYBR Premix Ex Taq (Tli RNase H Plus) kit (TaKaRa Bio Europe, Saint-Germain-enLaye, France) on a Realplex^2 Mastercycler Real-time PCR System (Eppendorf, Hamburg, Germany). Relative fold levels were determined using the 2(−DeltaDeltaCt) method [17], with GAPDH used as housekeeping control.

Orthotopic Xenograft Experiments

Animal experiments described were approved by the government of the state of North Rhine-Westphalia. Mice were maintained according to the guidelines of the Federation of European Laboratory Animal Science Associations. Orthotopic xenografts were generated by injecting 2.5×10^6 CDK5-F10 cells intradermally suspended in a total volume of 200 µl [PBS/Matrigel (BD Biosciences), 1:1 (v/v), prechilled to 4°C] into 6- to 8-week-old immunodeficient HPRT NOD-SCID mice (Jackson Laboratory, Maine, USA). After 2 weeks, subcutaneous tumor volumes were measured using digital calipers (Milomex, Pulloxhill, UK) and calculated using $V = 1/2(ab^2)$, where a is the longest and b is the shortest orthogonal tumor diameter [18]. Mice were then randomized and divided into two cohorts, one where mice received doxycycline (0.2 mg/ml) in drinking water containing 2.5% (w/v) sucrose to induce CDK5 knockdown *in vivo* and the control group where mice received only 2.5% (w/v) sucrose in drinking water. Tumor volumes and body weights were measured once weekly. After 5 weeks, tumors were harvested, and samples were snap-frozen or fixed in 10% buffered formalin for further analyses.

In vivo Lung Colonization Experiments

For this experimental metastasis assay, 6- to 8-week-old male immunodeficient HPRT NOD-SCID mice were used. First, 1×10^6 CDK5-F10 cells resuspended in 200 µl PBS were injected in the lateral tail vein. The group of mice designated CDK5-F10 (+dox) group was maintained on doxycycline (0.2 mg/ml), whereas the second group, designated CDK5-F10 (−dox), received water supplemented with sucrose only. After 10 weeks, mice were euthanized, and organs were harvested, fixed in 10% buffered formalin, and paraffin embedded. Hematoxylin-stained tissue sections were then evaluated histologically for the absence or presence of colonies formed by disseminated cancer cells within lungs and liver.

Syngenic Injection Model

Similarly, lung colonization assays were also done using an immunocompetent syngenic B16 murine model of melanoma. Briefly, 100,000 B16-shCDK5 and B16-shScr cells resuspended in 200 µl of PBS were injected in the tail vein of C57BL/6 mice. After 21 days, mice were euthanized, and the lungs and livers were fixed and paraffin embedded for further histological evaluation.

Phalloidin Staining

A total of 50,000 doxycycline-induced or -uninduced, stably transduced SKmel28 cells (clones F10 and B7) were seeded and grown on fibronectin (25 µg/ml)-coated 15-mm glass cover slips for 24 hours. On the next day, cells were washed with PBS and fixed with 4% formaldehyde for 20 minutes at room temperature. Cells were then permeabilized using 0.2% Triton X-100 (Sigma Aldrich) for 5 minutes followed by three washing steps with PBS. Fixed and permeabilized cells were then incubated with FITC-conjugated phalloidin (1:1000, Life Technologies) for 30 minutes at room temperature. Hoechst 33342 (Life Technologies) at a concentration of 1 µg/ml was used for staining of nuclei. Stained cells were then washed with PBS and mounted on glass slides using DAKO mounting medium. Images were captured using fluorescence microscopy.

Kinase Activity Assays

CDK5 kinase assays were performed as previously described elsewhere [10].

Statistical Analysis

Kruskal-Wallis analyses were carried out using SPSS version 11.0.1 for Microsoft Windows; two-tailed Student's t test and Mann-Whitney U test were performed using GraphPad Prism for Windows version 6. $P < .05$ was regarded as statistically significant. Unless indicated otherwise, results are shown as mean ± SD.

Results

Overexpression of CDK5 and its functional Activator CDK5R1/p35 in Human Melanoma

CDK5 has been described as ubiquitously expressed in mammalian tissues including melanoma cells [19], with its functional activity being regulated by and strictly dependent on its association with either one of its two activator proteins, CDK5R1/p35 or CDK5R2/p39, respectively. In other words, expression of either CDK5R1/p35 or CDK5R2/p39 is equivalent to CDK5 activation throughout various tissues [9,20–22]. Therefore, we evaluated p35 expression in human melanoma cells and primary tissue samples. Firstly, tissue microarrays (US Biomax, Inc., Rockville, MD) representing 86 cases of primary malignant melanoma lesions, 50 samples of melanoma metastases, and 27 control samples of normal skin tissue, with up to 3 replicates for each of the total 163 cases, were stained for p35 expression using immunohistochemistry. Each sample was scored as 0 (negative), 1+, 2+, or 3+ based on cytoplasmatic p35 immunolabeling; in cases with different values among replicate samples, the highest value was counted. Overexpression of p35 as compared with normal skin samples was found in 70% of melanoma tissues tested, including both primary and metastatic lesions. Thirty-six percent (49/136 cases) of melanomas (34 of 86 primary and 15 out of 50 metastatic lesions, respectively) showed high protein expression scored as "3+" as compared with basal immunolabeling (0 to 1+) observed in 100% (27 of 27 informative cases) of normal skin tissues. Intermediate (scored as "2+") expression was found in 34% (46/136 cases) of melanoma samples (31/86 primary and 15/50 metastatic melanoma lesions, respectively) but in none of the non-neoplastic normal skin control samples (Figure 1, *A* and *B*).

Next, we evaluated whether CDK5 activation by expression of p35 could be confirmed in melanoma cell lines cultured *in vitro* as well. Of note, constant strong basal protein expression of CDK5 was confirmed in all five melanoma cell lines (A375, SKMel28, FM8, Mel1479, DO8) tested in Western blot analyses, whereas expression of the CDK5-activator p35 and its cleavage product p25 was detected in four of five cell lines with considerable differences in basal expression levels. The highest steady-state expression levels were found in SKMel28 cells, which were therefore chosen for subsequent knockdown experiments (Figure 1*C*).

Inducible shRNA-Mediated Knockdown of CDK5 Inhibits Colony Formation and Anchorage-Independent Growth of Melanoma Cells In Vitro

To study the role of CDK5 in melanoma progression and metastasis, CDK5 function was abrogated using short hairpin RNA interference in melanoma cells. An inducible lentiviral pTRIPZ-Tet-On vector system was used for this purpose in which expression of shRNA is induced in the presence of doxycycline; red fluorescent protein served as control of transduction efficiency. SKMel28 melanoma cells were stably transduced with one of two independent CDK5-specific shRNA clones (designated "SKMel-F10" or "SKMel-B7," respectively) or with empty pTRIPZ vector as mock control. Transduction efficiency and specificity of doxycycline induction were tested using fluorescence microscopy (Figure 2*A*). Western blot analysis and quantitative real-time RT-PCR showed successful and reproducible knockdown of CDK5 upon addition of doxycycline in SKMel-F10 and SKMel-B7 mass clones at both the protein and mRNA level, but not in mock-transduced vector-only controls or in the absence of doxycycline (Figure 2*B*).

Of note, knockdown of CDK5 did not show any major effect on net cell growth of either of the tested melanoma cell clones for up to 72 hours in MTS assays, in line with previous reports stating that CDK5 is not directly involved in regulation of cell cycle progression (Figure 2*C*). As opposed to this, however, a rather pronounced effect of CDK5 knockdown on colony formation and anchorage-independent growth of SKMel melanoma cells was observed. Whereas addition of doxycycline did not affect colony formation of mock-transduced cells, marked inhibition was found in both SKMel-F10 and SKMel-B7 when comparing induced, shRNA-expressing cells to uninduced controls without addition of doxycycline. Moreover, colonies formed in SKMel-F10 or -B7 after CDK5 knockdown were found to be not only significantly fewer in numbers (reduction of colony counts by more than 90%) but also much smaller in average size (Figure 2*D*).

Suppression of CDK5 Impairs Migration and Invasiveness of Human Melanoma Cells

Cell motility and invasion are indispensable prerequisites for tumor progression and metastasis. CDK5 activation is known to be required for neuronal migration during brain development. Therefore, the potential role of CDK5 in cell motility and invasiveness of melanoma cells was studied using established *in vitro* model systems. Firstly, wound-healing assays were performed in near confluent monolayers of SKMel28 clones containing inducible CDK5-specific shRNA as described above, both in the presence or in the absence of doxycycline, respectively. Again, mock-transduced clones were included as additional controls alongside each set of experiments. The ability of cells to close the wound area was compared at 0 and 22 h. Of interest, mock controls as well as uninduced SKMel-F10 and SKMel-B7 clones migrated much faster into the scratch area and thus promoted quick closure of the wound gap as compared with their respective doxycycline-induced counterparts, thereby confirming the inhibitory effects of CDK5 knockdown on melanoma cell motility (Figure 3*A*). Migration and invasiveness were then assessed in

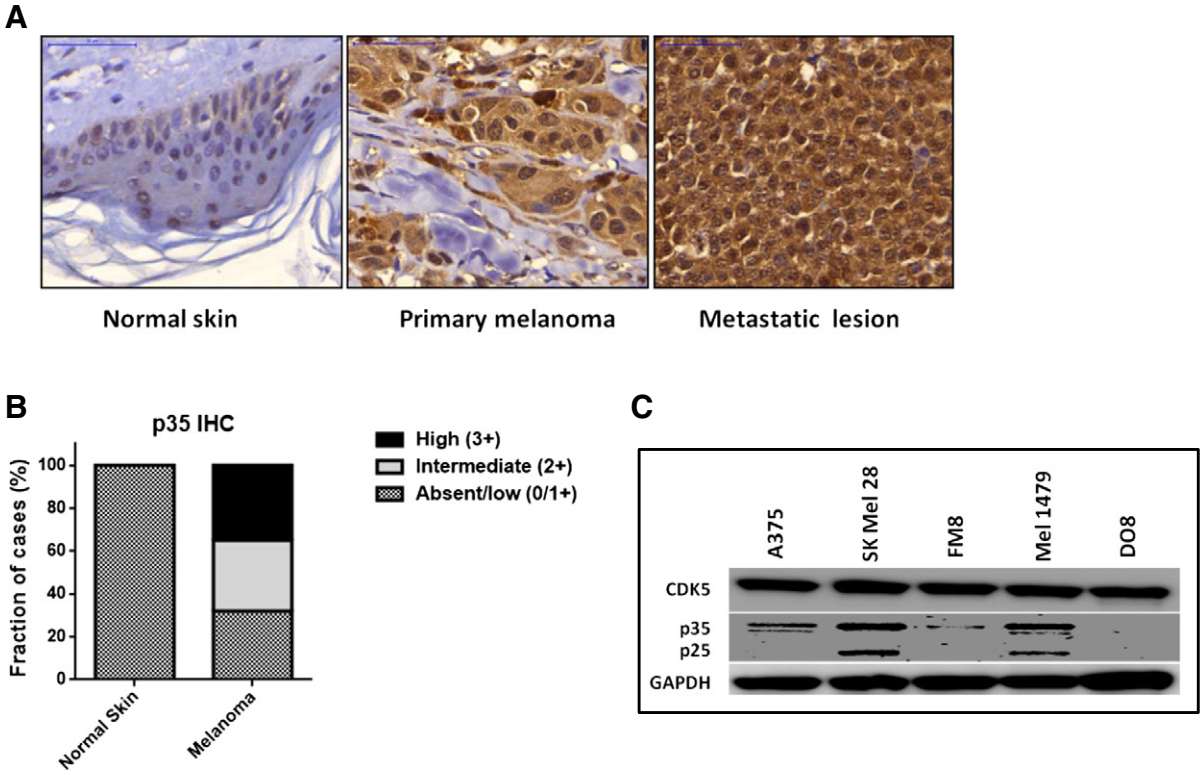

Figure 1. Expression of CDK5 and its activator protein CDK5R1/p35 in human melanoma tissues and cell lines. (A) CDK5R1/p35 was found to be overexpressed in primary melanoma as well as in metastatic lesions as compared with normal skin using immunohistochemistry. (B) In tissue microarrays, intermediate (2+) or high (3+) p35 immunolabeling was more commonly observed in malignant melanoma tissue as compared with benign skin. (C) Western blot analysis of CDK5, p35, and p25 steady-state expression levels in five human melanoma cell lines.

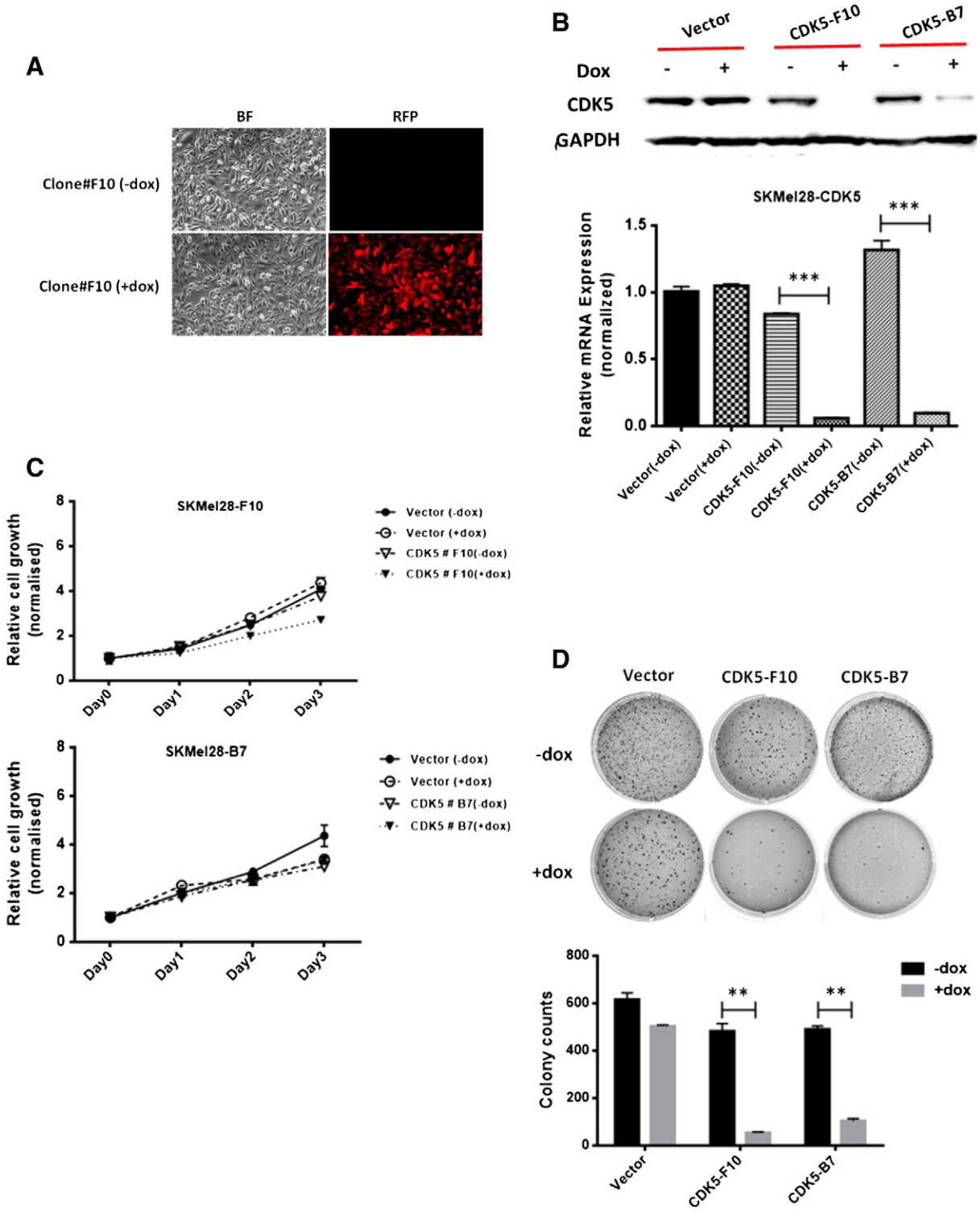

Figure 2. shRNA-mediated knockdown of endogenous CDK5 inhibits anchorage-independent growth of melanoma cells. An inducible pTRIPZ-Tet-On expression vector system containing CDK5-specific shRNA was used to knock down CDK5 expression in SKMel28 human malignant melanoma cells. (A) Transduction efficiency was confirmed by red fluorescent protein expression as visualized using fluorescence microscopy. (B) Successful inducible CDK5 knockdown was checked using Western blot analysis (upper panel) and quantitative real-time RT-PCR analysis (lower panel) both in the absence and in the presence of doxycycline, respectively. (C) Inducible knockdown of CDK5 did not show any significant effect on the net cell growth of SKMel28 cells as assessed using MTS assay. The figure shows results of two different pairs of mass clones (designated "SKMel28-F10" and SKMel28-B7" with their respective mock controls) both in the presence (= induced state) and in the absence (= uninduced state) of doxycycline. (D) In contrast, colony formation and anchorage-independent growth in soft agar were significantly reduced in both SKMel28 mass clones when induced by doxycycline as compared with uninduced or mock-transduced controls. Colony counts are plotted as means and SD from three independent experiments; $*P < .05$.

modified Matrigel-coated Boyden chamber assays. SKMel-F10 and SKMel-B7 cells or respective mock-transduced controls were plated into the bottoms of the transwell inserts and allowed to invade through a Matrigel layer as a surrogate for extracellular matrix, again both in the presence and in the absence of doxycycline, over a period of 72 hours. Notably, CDK5 knockdown led to marked reduction of invasion/migration in this model. Doxycycline stimulation did not have any apparent effect on mock-transduced controls, ruling out unspecific cytotoxic effects (Figure 3*B*).

Loss of CDK5 Expression Affects Morphology and Adhesion of melanoma Cells

In neuronal progenitor cells as well as in other cancer types, CDK5 depletion was found to cause significant changes in cell morphology and to profoundly affect actin cytoskeleton reorganization [9,23,24]. Therefore, we next examined whether the observed effects on melanoma cell migration following CDK5 knockdown might be due to modulation of cytoskeleton reorganization as demonstrated using immuofluorescence labeling of F-actin fibers. Both uninduced SKMel-F10 or B7 clones as well as mock transduced clones showed marked cell spreading and tight attachment to fibronectin-coated surfaces. Also, cells were more motile and regularly formed well-defined pseudopodia. In contrast, doxycycline-induced, CDK5-depleted cells showed randomly oriented actin fibers with no discernible polarity, were smaller in size, and showed decreased ability to protrude and spread on the coated surface (Figure 3*C*).

Our *in vitro* results thus hint at a possible involvement of CDK5 in melanoma cell motility, invasion, and cytoskeleton reorganization. Therefore, we next tried to assess whether changes in CDK5 functional activity might play a role in melanoma progression and metastatic spread using suitable *in vivo* model systems.

CDK5 Knockdown Inhibits Orthotopic Melanoma Xenograft Growth

To generate orthotopic xenografts, 2×10^6 SKMel-F10 melanoma cells were injected intradermally into the flanks of female NOD-SCID mice and allowed to grow for 2 weeks, at which point average tumor volumes reached approximately 80 mm^3. Mice were

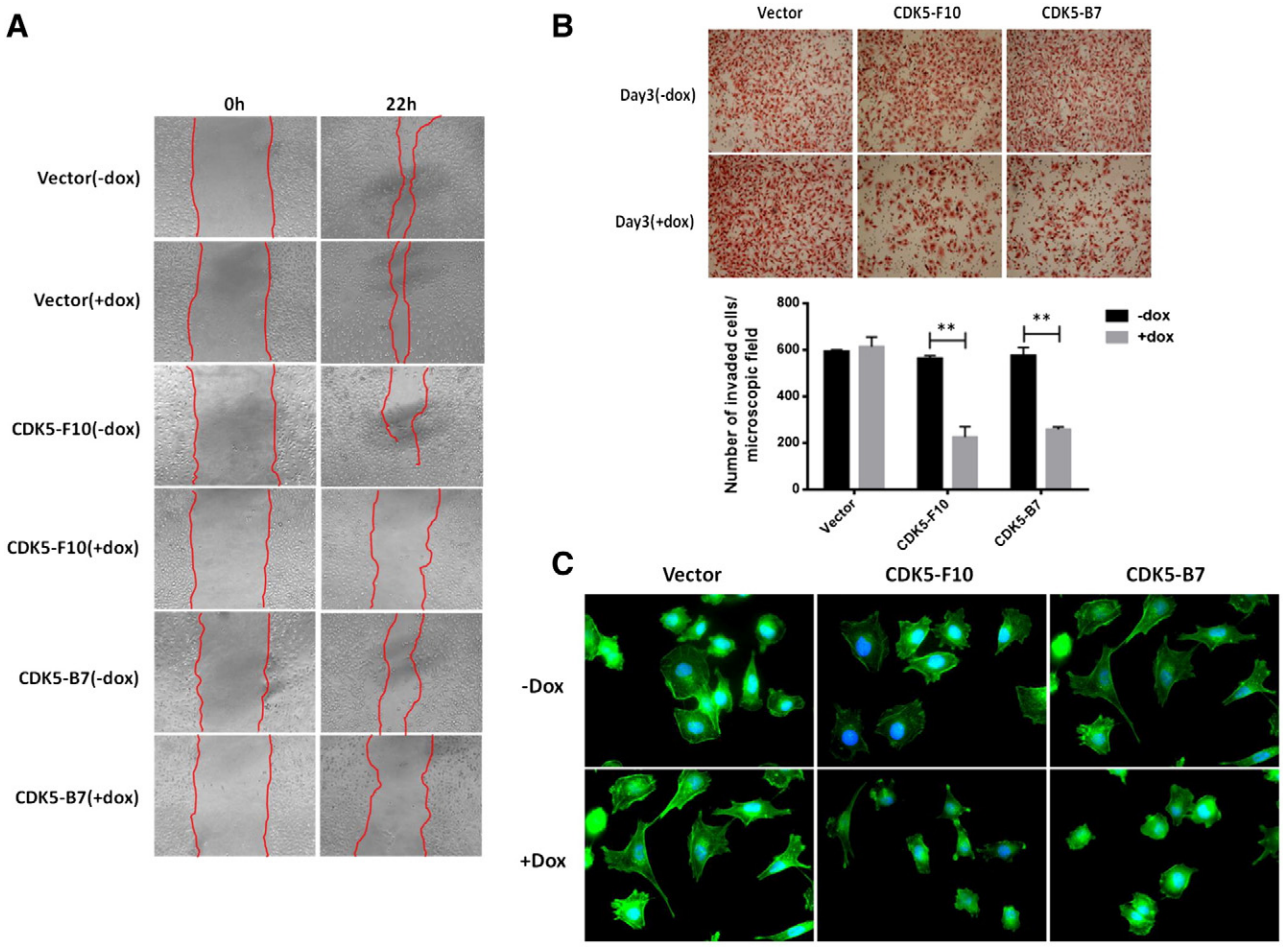

Figure 3. Abrogation of CDK5 inhibits melanoma cell motility and invasiveness. (A) Wound-healing assays were performed in either mock-transduced or CDK5-shRNA–expressing SKMel28 clones with or without addition of doxycycline, respectively. The ability of cells to migrate and close the wound area after 22 hours was compared. (B) Modified Boyden chamber assay revealed significantly reduced invasion and migration through Matrigel of SKMel28 cells upon doxycycline-induced shRNA-mediated knockdown of CDK5. The bar diagram shows relative cell counts as means and SD. $^{**}P < .01$ (C) Induced knockdown of CDK5 expression influenced cell morphology and impaired cytoskeleton remodeling as shown by immunofluorescence labeling of F-actin by phalloidin. Both SKMel-F10 and B7 cells lacked F-actin bundles and showed a loss of cell polarity in the presence of doxycycline, whereas no such effect was observed in uninduced and mock-transduced clones.

then randomly assigned to either one of two study arms: The first group received doxycycline (200 μg/ml) and sucrose (2.5% w/v) in their drinking water continuously for the following 5 weeks, whereas the second group received only sucrose without addition of doxycycline. Of note, the group of mice in which CDK5 knockdown was induced (CDK5-F10 + dox) showed significantly inhibited tumor growth as compared with uninduced controls with preserved CDK5 expression (Figure 4*A*). Neither loss in body weight nor any other signs of distress or behavioral abnormalities were observed in mice from either of the two groups during the entire experiment. After 5 weeks, tumors were harvested, and persistent knockdown of CDK5 was confirmed by Western blot analysis (Figure 4*B*) as well as by immunohistochemistry (Figure 4*C*). Proliferation was assessed using Ki-67 labeling, and no discernible differences were found between the two arms, in line with *in vitro* data presented above. Also, no discernible histological differences were observed between xenografts derived from the CDK5 knockdown or control arm, respectively (Figure 4*C*).

CDK5 Knockdown Inhibits Formation of Lung and Liver Metastases in a Murine Injection Model of Human Melanoma

Next, we aimed to further evaluate these promising *in vivo* data using a complementary second *in vivo* model system, this time specifically mimicking the formation of systemic metastases. For this end, SKMel-F10 cells were injected into the tail veins of NOD-SCID mice. CDK5 knockdown was then induced *in vivo* by addition of doxycycline in drinking water, whereas uninduced mice served as controls. Interestingly, in this scenario, CDK5 blockade almost completely abrogated formation of lung colonies: uninduced SKMel-F10 cells formed multiple pulmonary lesions in all animals that were readily identified by gross inspection or histopathological examination, whereas doxycycline-induced CDK5-depleted melanoma cells yielded significantly fewer lesions of minimal size (Figure 5*A*). Again, these observations were reproducible in several sets of experiments and in line with *in vitro* data presented above.

Inhibition of CDK5 Activity by Means of shRNA-Mediated Knockdown Blocks Lung Colonization Reminiscent of Pulmonary Metastases in a Syngenic Murine Melanoma Injection Model

To complement our experimental *in vivo* data obtained in xenogenic transplantation models with immunocompromised mice, we aimed to further validate the observed inhibition of metastatic spread through abrogation of CDK5 in a third, syngenic *in vivo* model system with fully immunocompetent wild-type mice. For this, the murine melanoma cell line B16F10 was used, in which CDK5 knockdown was achieved using a sequence-specific shRNA (Figure 5*B*). Scrambled shRNA was applied for mock transduction. Injection of B16F10 murine melanoma cells stably transduced with murine CDK5 shRNA (B16-CDK5#1) into tail veins of C57/BL6 mice reproducibly led to diminished formation of pulmonary metastases as compared with mock clones. Since the used B16 cell line expresses high levels of melanin, these lesions were readily visible upon gross inspection (Figure 5*C*). Histopathological examination confirmed large fulminant metastatic lesions in the lungs of mice injected with B16-sh scrambled cells as compared to markedly reduced lung metastases in mice injected with B16-shCDK5#1.

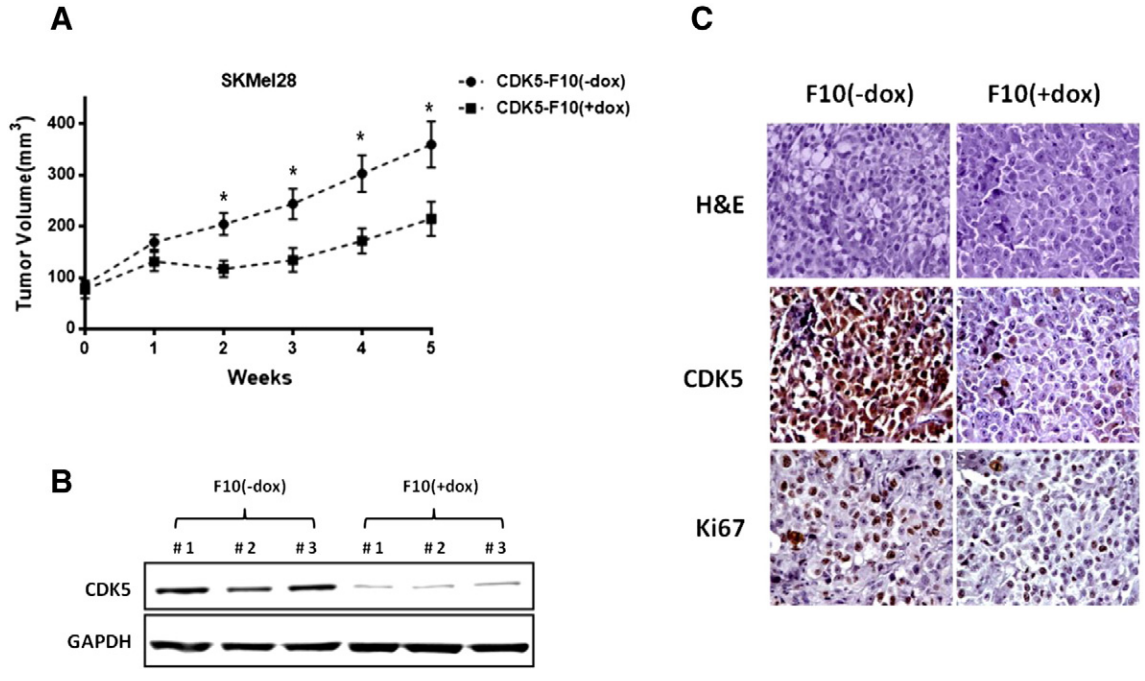

Figure 4. Inhibition of CDK5 function through shRNA-mediated knockdown impairs *in vivo* tumorigenicity in orthotopic melanoma xenografts. (A) Growth of orthotopic SKMel-F10 xenografts was significantly inhibited upon induced CDK5 knockdown. (B) Sustained induced CDK5 knockdown was confirmed in explanted xenograft tumor tissues at the end of the experiment using Western blot analysis. Results from three representative doxycycline-induced and -uninduced mock-treated xenografts, respectively, are shown. (C) H&E stainings did not reveal any major discernible changes in the tumor microarchitecture upon induced CDK5 knockdown. Immunohistochemistry in harvested xenograft tumor tissues confirmed efficient knockdown of CDK5 at the protein level; proliferation as determined by Ki-67 immunolabeling was not significantly reduced after CDK5 depletion.

Thus, consistent with the phenotypic effects observed *in vitro*, our data provide strong evidence that inhibition of CDK5 is associated with strong blockade of melanoma progression and metastasis in all of the three *in vivo* model systems used here.

CDK5 Inactivation Leads to Upregulation and Dephosphorylation of Caldesmon

Activity of the actin- and calmodulin-binding protein caldesmon is modulated via phosphorylation. In its dephosphorylated state, caldesmon binds to and stabilizes actin filaments, inhibits cell migration, and suppresses formation of podosomes and invadopodia [25–29]. Therefore, a possible involvement of caldesmon in the phenotype observed in CDK5-depleted melanoma cells as described above was examined.

Of interest, it was found that doxycycline-induced depletion of CDK5 in either SKMel-F10 or -B7 cells led to dephosphorylation of caldesmon while at the same time causing an increase of total caldesmon as observed using Western blot analysis. No change in phosphorylation status was found in uninduced SKMel-F10 or -B7 cells or in mock-transduced controls (Figure 6*A*).

siRNA-Mediated Knockdown of Caldesmon Rescues Cell Motility and Invasion/Migration in CDK5-Depleted Melanoma Cells

To test whether upregulation and dephosphorylation of caldesmon might indeed be an underlying cause of the observed phenotype in CDK5-depleted melanoma cells with decreased cell motility and invasion/migration as surrogate for an overall decrease in their metastatic potential, rather than just a bystander effect, rescue experiments were carried out. For this, SKmel-F10 cells were transfected with scrambled or caldesmon-specific siRNA (siGenome smartpool siRNA; 25 nM) and assayed for their migratory and invasive ability using modified Boyden chamber and wound-healing assays. Successful RNAi-mediated knockdown of caldesmon in both doxycycline-induced and -uninduced SKmel-F10 cells was confirmed by Western blot analysis (Figure 6*B*). Interestingly, in CDK5-deficient melanoma cells, invasion and migration were significantly rescued by caldesmon depletion as observed using modified Boyden chamber and wound-healing assays. Invasion and migration of uninduced cells (SKMel-F10 – dox) on the other hand were not affected when depleted of caldesmon ("+siCald") as compared with scrambled controls ("+siScr") (Figure 6, *C* and *D*).

Melanoma Cell Migration/Invasion and Colony Formation Are Readily Inhibited by Pharmacological Blockade of CDK5 Activity

Having identified CDK5 as a promising molecular target for therapeutic intervention in melanoma using genetic *in vitro* and *in vivo* model systems as described above, we next wanted to evaluate if these therapeutic effects could be replicated by pharmacological

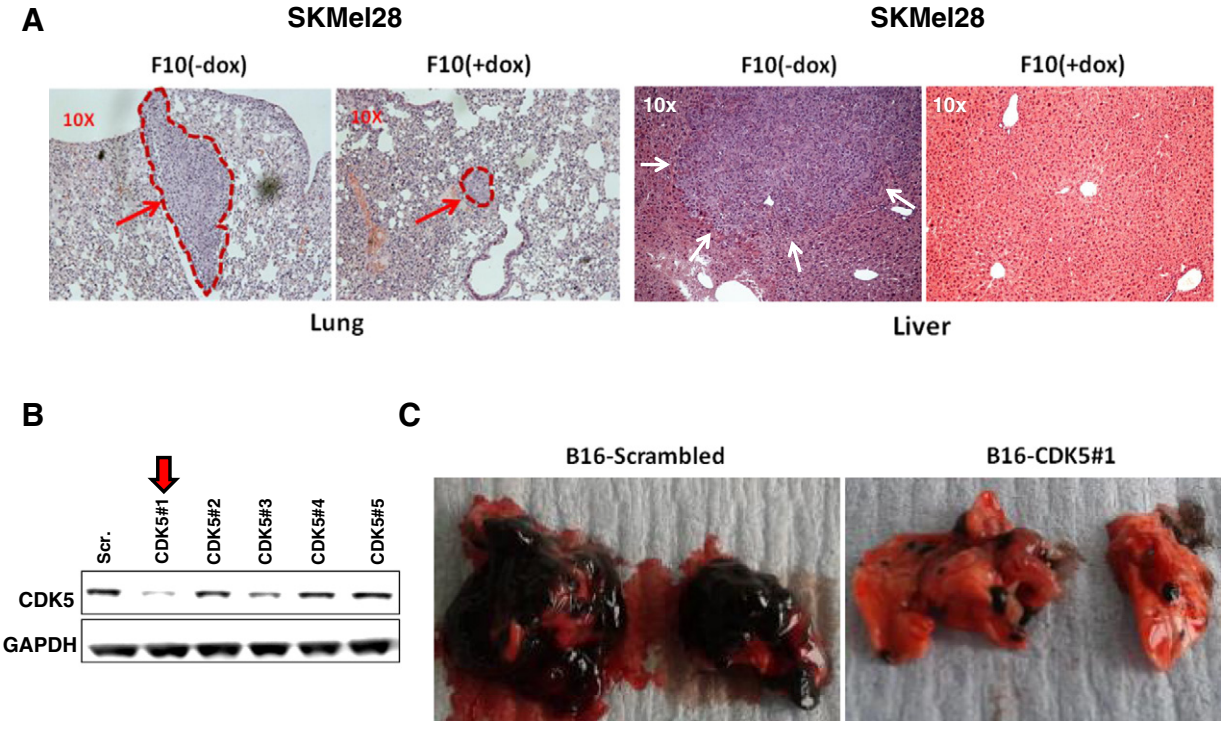

Figure 5. CDK5 knockdown prevents metastatic melanoma spread in murine dissemination models. (A) Formation of lung and liver metastases after intravenous injection of SKMel28 melanoma cells in immunodeficient HPRT NOD-SCID mice was determined. In this model system, doxycycline-induced shRNA-mediated CDK5 knockdown led to a dramatic reduction in the average number and size of pulmonary lesions as compared with uninduced controls (left panel). Liver metastases were completely abolished upon induced CDK5 knockdown, whereas they were readily observed in uninduced controls (right panel). The figures show representative H&E stains of FFPE tissue sections. (B) Injection of B16 murine melanoma cells into the tail veins of C57BL/6 wild-type mice was applied as a third, syngenic *in vivo* model system to validate the effect of CDK5 abrogation on melanoma metastasis. One of five CDK5-specific shRNA-clones ("CDK5#1") showed reproducible knockdown of CDK5 in B16 murine melanoma cells as compared with scrambled controls using Western blot analysis. (C) When this clone CDK5#1 was used in a tail vein injection model, a dramatic decrease in both the amount and average size of lung colonies representing pulmonary metastases was observed upon CDK5 knockdown as compared to mock-transfected cells (macroscopic image from two representative animals).

inhibition of CDK5 as well. To this end, a series of novel small molecule inhibitors was screened for their ability to bind CDK5 and block its kinase activity [30]. *N*-(5-isopropylthiazol-2-yl)-3-phenylpropanamide (PJB) (Pubchem CID = 16760027) (Figure 7*A*) was found to potently inhibit CDK5 activity in kinase assays (Figure 7*B*), which is in line with previous observations, which had shown an IC50 of around 64 nM for CDK5 and 98 nM for CKD2 inhibition, respectively [31,32]. For subsequent efficacy testing, PJB was used alongside the well-established yet less specific small molecule CDK5 inhibitor roscovitine.

Of note, and in line with data obtained from CDK5 knockdown experiments, CDK5 inhibition with roscovitine or PJB did not have any discernible effect on net cell viability as assessed using MTS assays at concentrations of up to 10 μM after up to 72 hours (Figure 8*A*).

However, in modified Boyden chamber assays, pharmacological CDK5 inhibition with either roscovitine or PJB led to near-complete inhibition of invasion/migration of SKMel28 melanoma cells, reminiscent of effects observed in the previously described genetic model systems of CDK5 inhibition (Figure 8*B*). Finally, as opposed to net cell growth as observed in MTS assays, *in vitro* colony

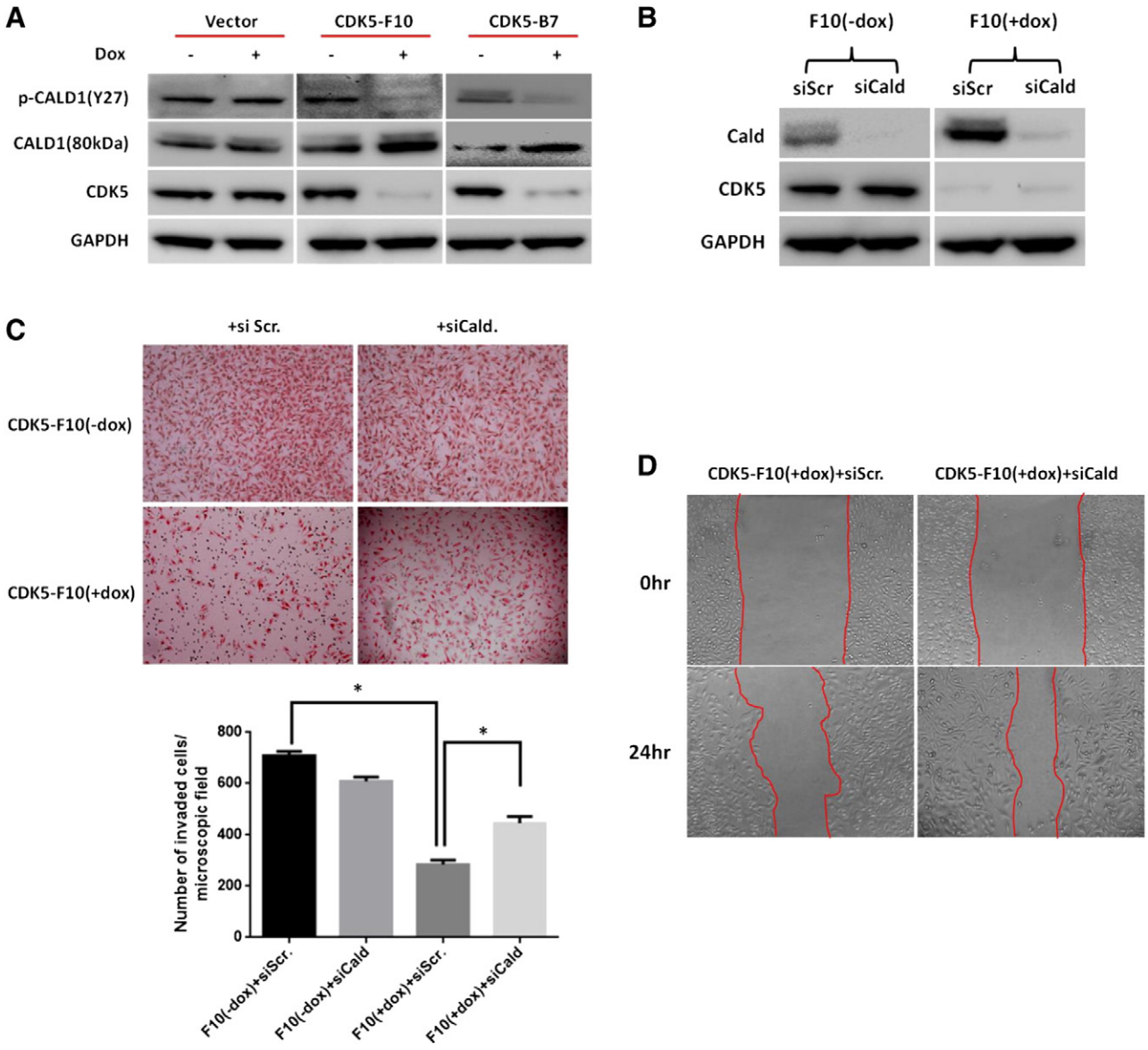

Figure 6. CDK5 affects melanoma invasiveness and migration through regulation of caldesmon. (A) shRNA-mediated knockdown of CDK5 causes upregulation and dephosphorylation of caldesmon in SKMel-F10 and SKMel-B7 cells in the presence of doxycycline as compared with uninduced or mock-transduced cells as demonstrated using Western blot analysis. (B) Successful siRNA-mediated knockdown of caldesmon is demonstrated in CDK5 knockdown cells. Note that CDK5 protein levels are not affected by caldesmon knockdown. (C) Caldesmon knockdown rescues invasiveness and migration of CDK5-depleted SKMel human melanoma cells. The upper panel shows membranes from modified Boyden chamber assays; loss of invasion/migration upon doxycycline-induced CDK5 knockdown is rescued by concomitant siRNA-mediated knockdown of caldesmon, whereas no effect is found in scrambled siRNA controls. Relative cell counts as means and standard deviations are shown in the lower panel. *$P < .05$. (D) In wound-healing assays, concomitant caldesmon knockdown by means of siRNA transfection leads to increased cell motility, thus rescuing the observed reduction in wound healing upon downregulation of CDK5 as shown above.

formation of SKMel28 melanoma cells and anchorage-independent growth in soft agar were abrogated upon CDK5 inhibition by roscovitine or PJB as well (Figure 8*C*).

Of note, similar to what was seen in the genetic model, SKMel melanoma cells treated with roscovitine or PJB also showed no significant change (roscovitine) or a slight increase (PJB) in total caldesmon protein levels, whereas phosphorylation of caldesmon was decreased using either of the two compounds (Figure 8*D*).

Discussion

Although localized melanoma is effectively treated by local intervention such as surgical resection or irradiation, therapeutic options and overall prognosis for metastatic disease remain poor to date despite tangible progress in recent years such as the advent of novel tyrosine kinase inhibitor–based targeted or immunomodulatory therapies.

CDK5 has been well established as centrally involved in regulating migration of neuronal progenitor cells during brain development in embryogenesis [20,33,34], whereas extraneuronal reactivation of CDK5 in malignant tumors has only recently been recognized. Our data presented here provide strong experimental evidence that activation of CDK5 by overexpression of its activator p35 mediates invasive properties and metastatic spread in malignant melanoma and suggest CDK5 as potential therapeutic target for therapies aimed at inhibiting metastasis in this disease. This was shown in primary human tissue samples as well as in cell lines derived from melanoma patients. From a translational point of view, it has been difficult in the past to predict clinical relevance of putative therapeutic targets based on preclinical experimental data, possibly because specific experimental conditions used in a particular model system can often greatly influence the obtained results [35]. Therefore, in this present study, particular efforts were made to corroborate the observed phenotype of decreased invasive and migratory potential of CDK5 depletion in melanoma cells using various redundant *in vitro* as well as three different *in vivo* model systems as described above, thus increasing the chance of describing a target that will indeed prove to be relevant in future clinical trials.

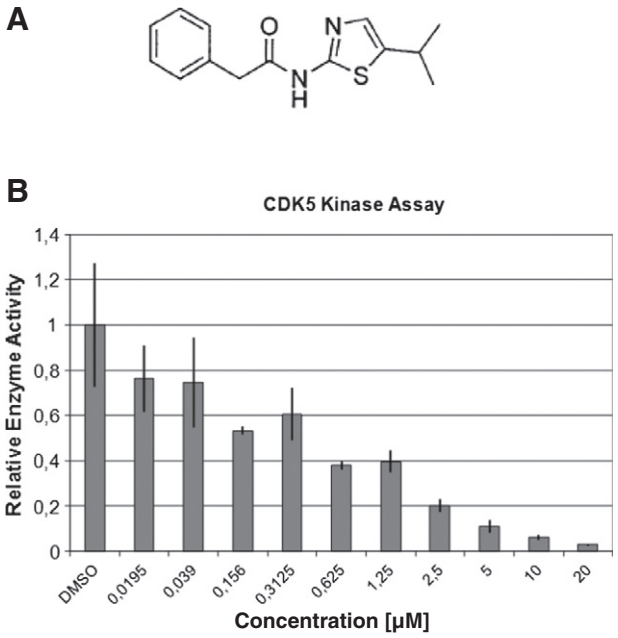

Figure 7. PJB as small molecule CDK5 inhibitor. (A) Chemical structure of PJB. (B) Kinase assays show dose-dependent inhibition of CDK5 kinase activity by PJB.

It is important to note that abrogation of CDK5 signaling through shRNA-mediated knockdown had profound effects on melanoma cell migration and invasion *in vitro* that were mirrored by loss of metastatic potential across three different *in vivo* model systems used here, while at the same time apparently not directly affecting cell growth both *in vitro* and *in vivo*. Recently, various groups, including our own, have begun to accumulate experimental evidence supporting a potential role of CDK5 in the progression of different cancers [9,10,18]. In prostate cancer, CDK5 activity has been shown to be involved in metastatic spread and has been suggested as possible drug target for therapeutic intervention [10,11,36]. CDK5 is functionally active in pancreatic cancer as well and was found to be amplified in a subset of cases [37]. We as well as others found it to contribute to tumor progression, and it has been suggested as a therapeutic target that potentially allows modulation of oncogenic Kras downstream effector signaling axes such as the RalGDS-Ral pathway [9,18,37]. Of note, a recent study reports that inhibition of CDK5 activity in combination with pharmacological AKT inhibition showed a dramatic therapeutic response in preclinical animal models that led to initiation of a phase 1 clinical trial currently evaluating this promising novel approach in humans [38].

Likewise, increased CDK5 activity was found in hepatocellular carcinoma, and CDK5 was identified as a potential therapeutic target for hepatocellular carcinoma with potential synergism with DNA damage response pathways [39].

In a recent report, CDK5 expression and activation in approximately 50% of esophageal squamous cell carcinoma samples have been described and were linked to distinct subsets of tumors with adverse prognosis and enhanced expression of the stem cell marker nestin [40].

In medullary thyroid carcinoma (MTC), CDK5 activity has been suggested to be involved in control of tumor cell proliferation through phosphorylation and activation of STAT3 [41]. Of interest, in a more recent study, Pozo et al. were able to show that activation of CDK5 by C cell–specific overexpression of its activator p25, a cleavage product of CDK5R1/p35, was sufficient to induce formation of MTC in a conditional mouse model. Using this setup, the authors were able to show that, in this context, aberrantly activated CDK5 signals via retinoblastoma, thus influencing initiation and progression of MTC [42]. Using this model, CDK5 was described as a tumor-initiating factor and a potential therapeutic target in MTC [43].

In multiple myeloma, CDK5 has been identified as an adverse prognostic marker and was proposed to confer resistance towards proteasome inhibitors bortezomib and carfilzomib [44]. Moreover, the multikinase inhibitor dinaciclib, which among others blocks CDK5 activity with high affinity, has recently been found to be therapeutically active as a single-agent monotherapy in highly pretreated multiple myeloma [45]. In leukemia cells, CDK5 was found to phosphorylate and functionally inhibit the proapoptotic protein Noxa [46]. Of interest, CDK5 has recently been suggested to regulate the tumor suppressor DLC1 by phosphorylation in lung adenocarcinoma [47]. Finally, in mantle cell lymphoma samples, CDK5 has been described as overexpressed due to promoter hypomethylation [48].

More recently, aberrant CDK5 signaling was suggested to be involved in migration of endothelial cells, lymphangiogenesis, and formation of blood vessels [49,50].

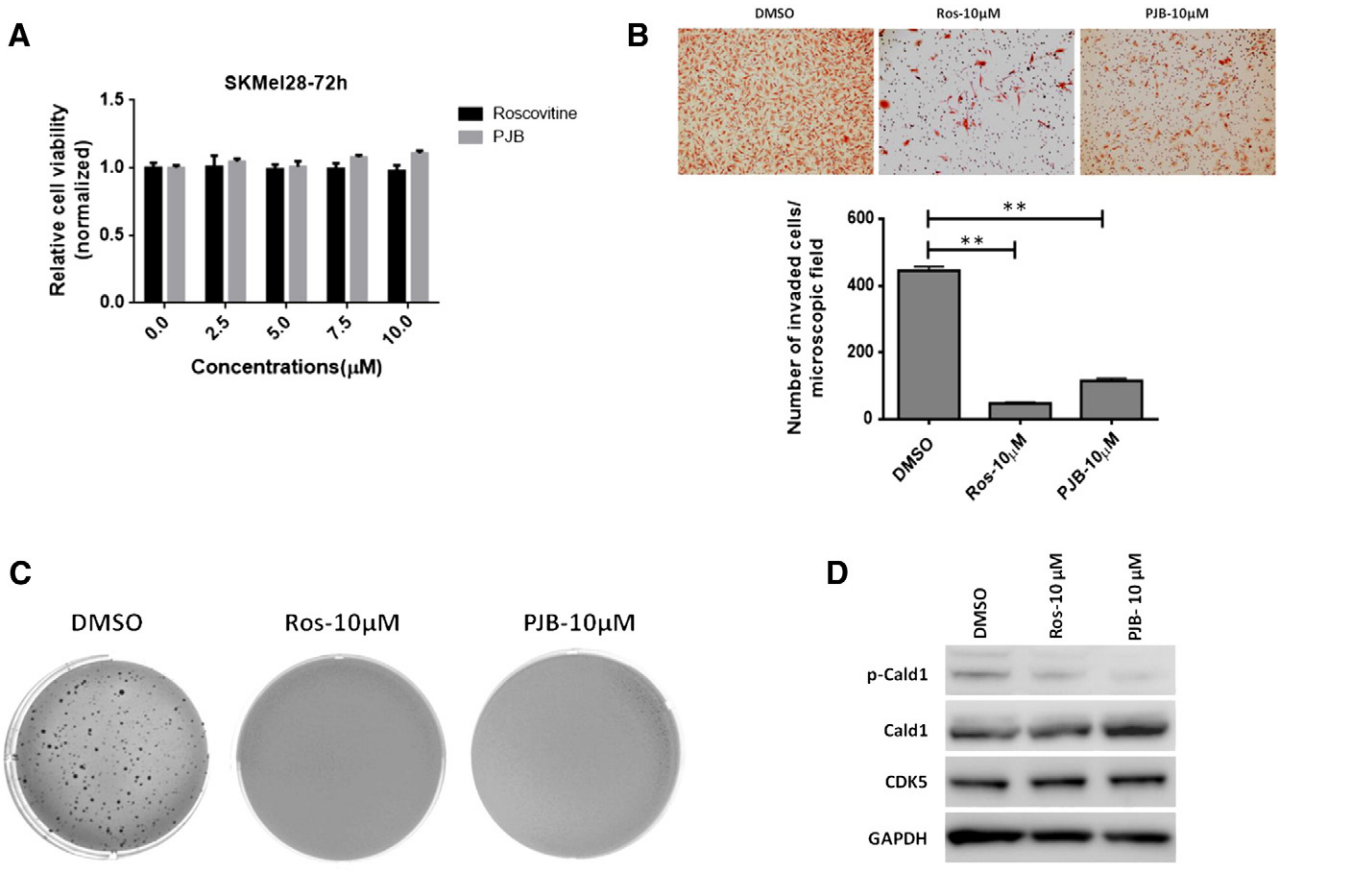

Figure 8. Therapeutic *in vitro* efficacy testing of pharmacological inhibition of CDK5 activity. (A) MTS assays do not show any reduction in cell viability after 72 hours upon incubation with up to 10 μM roscovitine or PJB. (B) Reduction of invasion/migration in modified Boyden chamber assays and of (C) colony formation and anchorage-independent growth in soft agar assays upon CDK5 inhibition with roscovitine or PJB, respectively. (D) Small molecule CDK5 inhibitors roscovitine or PJB caused dephosphorylation of caldesmon, while not affecting total CDK5 protein levels as observed using Western blot analysis.

Together, these data show that, apart from its known physiological roles in regulation of neuronal migration during brain development, CDK5 is increasingly recognized as being involved in several additional, extraneuronal pathophysiological functions. CDK5 being a highly pleiotropic protein, the studies published on this topic, some of which are cited above, name a currently rapidly growing number of diseases in which aberrant CDK5 activation apparently plays a crucial role and unmask a variety of potential underlying mechanisms and signaling pathways involved. With respect to malignant tumors, the emerging common underlying theme seems to be that of CDK5 being a protein kinase driving tumor progression and metastasis across various malignancies via several different mechanisms in a highly tissue-specific manner.

This current study for the first time provides experimental evidence based on primary tumor samples as well as clinically relevant *in vitro* and *in vivo* model systems for proinvasive and prometastatic effects of activated CDK5 in melanoma cells. Moreover, phosphorylation of caldesmon is uncovered as a potential underlying mechanism in this case. Of note, in addition to phosphorylation of caldesmon at Tyr27 as demonstrated here, several other phosphorylation sites of caldesmon have been previously described [51], and one might speculate that these could also represent potential targets of CDK5, opening up interesting avenues for future work. Caldesmon has previously been shown to bind and thereby stabilize actin filaments, which are antagonized by cell cycle–dependent phosphorylation of caldesmon on specific serine and threonine residues [52,53]. Tyrosine phosphorylation of caldesmon has been found to cause its dissociation from actin, thereby contributing to actin microfilament disassembly [54,55]. In a recent study by Boerner et al., only phosphotyrosine-27 of caldesmon was found to be required for binding to either the amino-terminal SH3 or central SH2 domains of Grb2 [56]. Our data are in line with a recent report by Quintavalle et al. suggesting that CDK5 has the potential to directly phosphorylate caldesmon in src-3 T3 and SCC61 cells, thereby inhibiting cytoskeleton remodeling, formation of invadopodia, and invasive behavior [51]. The authors of that study also conclude that CDK5 might be exploited as a molecular target for therapeutic intervention with the potential to block metastatic spread, similar to conclusions drawn in our own study on CDK5 activation in malignant melanoma. Indeed, a novel small molecule CDK5 inhibitor, PJB, was found to inhibit *in vitro* melanoma cell migration/invasion, colony formation, and anchorage-independent growth as correlate of tumor progression. Therefore, further studies evaluating therapeutic *in vivo* efficacy of this novel compound using suitable small animal models will be of interest.

Following up on the idea to use CDK5 as drug target in melanoma appears even more intriguing since other suitable CDK5 small molecule inhibitors are currently already under development and or in early clinical testing for other indications [11,45,57,58]. Therefore,

it is very likely that suitable drugs with known dosing schedules, pharmacokinetics data, and toxicity profiles might soon be available, which could then relatively easily and safely be evaluated in patients suffering from metastatic melanoma.

Conclusion

This study provides strong experimental evidence for an involvement of CDK5 activity in metastatic spread of malignant melanoma, possibly via modulation of caldesmon phosphorylation. With pharmacological CDK5 inhibitors currently already being developed for other indications and tested with respect to their pharmacokinetics and toxicity profiles, this might open up a viable opportunity for therapeutic intervention aimed at blocking melanoma metastasis in the near future.

Acknowledgements

This work was supported in part by the European Community's Seventh Framework Program [FP7-2007-2013] under grant agreement HEALTH-F2-2011-256986, by the German Cancer Foundation (Deutsche Krebshilfe) grant numbers 109215 and 109929 to G.F., as well as by the University Hospital of Bonn, BONFOR grant number O-142.0005 to S.B.

References

[1] Siegel R, Ma J, Zou Z, and Jemal A (2014). Cancer statistics, 2014. *CA Cancer J Clin* **64**(1), 9–29.

[2] Brahmer JR, Tykodi SS, Chow LQ, Hwu WJ, Topalian SL, Hwu P, Drake CG, Camacho LH, Kauh J, and Odunsi K, et al (2012). Safety and activity of anti-PD-L1 antibody in patients with advanced cancer. *N Engl J Med* **366**(26), 2455–2465.

[3] Topalian SL, Hodi FS, Brahmer JR, Gettinger SN, Smith DC, McDermott DF, Powderly JD, Carvajal RD, Sosman JA, and Atkins MB, et al (2012). Safety, activity, and immune correlates of anti–PD-1 antibody in cancer. *N Engl J Med* **366**(26), 2443–2454.

[4] Lito P, Pratilas CA, Joseph EW, Tadi M, Halilovic E, Zubrowski M, Huang A, Wong WL, Callahan MK, and Merghoub T, et al (2012). Relief of profound feedback inhibition of mitogenic signaling by RAF inhibitors attenuates their activity in BRAFV600E melanomas. *Cancer Cell* **22**(5), 668–682.

[5] Sullivan RJ, Lorusso PM, and Flaherty KT (2013). The intersection of immune-directed and molecularly targeted therapy in advanced melanoma: where we have been, are, and will be. *Clin Cancer Res* **19**(19), 5283–5291.

[6] Xie Z, Sanada K, Samuels BA, Shih H, and Tsai LH (2003). Serine 732 phosphorylation of FAK by Cdk5 is important for microtubule organization, nuclear movement, and neuronal migration. *Cell* **114**(4), 469–482.

[7] Contreras-Vallejos E, Utreras E, and Gonzalez-Billault C (2012). Going out of the brain: non-nervous system physiological and pathological functions of Cdk5. *Cell Signal* **24**(1), 44–52.

[8] Banks AS, McAllister FE, Camporez JP, Zushin PJ, Jurczak MJ, Laznik-Bogoslavski D, Shulman GI, Gygi SP, and Spiegelman BM (2014). An ERK/Cdk5 axis controls the diabetogenic actions of PPARgamma. *Nature* **517**, 391–395

[9] Feldmann G, Mishra A, Hong SM, Bisht S, Strock CJ, Ball DW, Goggins M, Maitra A, and Nelkin BD (2010). Inhibiting the cyclin-dependent kinase CDK5 blocks pancreatic cancer formation and progression through the suppression of Ras-Ral signaling. *Cancer Res* **70**(11), 4460–4469.

[10] Strock CJ, Park JI, Nakakura EK, Bova GS, Isaacs JT, Ball DW, and Nelkin BD (2006). Cyclin-dependent kinase 5 activity controls cell motility and metastatic potential of prostate cancer cells. *Cancer Res* **66**(15), 7509–7515.

[11] Wissing MD, Dadon T, Kim E, Piontek KB, Shim JS, Kaelber NS, Liu JO, Kachhap SK, and Nelkin BD (2014). Small-molecule screening of PC3 prostate cancer cells identifies tilorone dihydrochloride to selectively inhibit cell growth based on cyclin-dependent kinase 5 expression. *Oncol Rep* **32**(1), 419–424.

[12] van Kuppeveld FJ, van der Logt JT, Angulo AF, van Zoest MJ, Quint WG, Niesters HG, Galama JM, and Melchers WJ (1992). Genus- and species-specific identification of mycoplasmas by 16S rRNA amplification. *Appl Environ Microbiol* **58**(8), 2606–2615.

[13] Kutner RH, Zhang XY, and Reiser J (2009). Production, concentration and titration of pseudotyped HIV-1-based lentiviral vectors. *Nat Protoc* **4**(4), 495–505.

[14] Feldmann G, Dhara S, Fendrich V, Bedja D, Beaty R, Mullendore M, Karikari C, Alvarez H, Iacobuzio-Donahue C, and Jimeno A, et al (2007). Blockade of hedgehog signaling inhibits pancreatic cancer invasion and metastases: a new paradigm for combination therapy in solid cancers. *Cancer Res* **67**(5), 2187–2196.

[15] Mullendore ME, Koorstra JB, Li YM, Offerhaus GJ, Fan X, Henderson CM, Matsui W, Eberhart CG, Maitra A, and Feldmann G (2009). Ligand-dependent Notch signaling is involved in tumor initiation and tumor maintenance in pancreatic cancer. *Clin Cancer Res* **15**(7), 2291–2301.

[16] Haan C and Behrmann I (2007). A cost effective non-commercial ECL-solution for Western blot detections yielding strong signals and low background. *J Immunol Methods* **318**(1-2), 11–19.

[17] Livak KJ and Schmittgen TD (2001). Analysis of relative gene expression data using real-time quantitative PCR and the 2(−Delta Delta C(T)) Method. *Methods* **25**(4), 402–408.

[18] Feldmann G, Mishra A, Bisht S, Karikari C, Garrido-Laguna I, Rasheed Z, Ottenhof NA, Dadon T, Alvarez H, and Fendrich V, et al (2011). Cyclin-dependent kinase inhibitor dinaciclib (SCH727965) inhibits pancreatic cancer growth and progression in murine xenograft models. *Cancer Biol Ther* **12**(7), 598–609.

[19] Abdullah C, Wang X, and Becker D (2011). Expression analysis and molecular targeting of cyclin-dependent kinases in advanced melanoma. *Cell Cycle* **10**(6), 977–988.

[20] Dhavan R and Tsai LH (2001). A decade of CDK5. *Nat Rev Mol Cell Biol* **2**(10), 749–759.

[21] Tsai LH, Delalle I, Caviness Jr VS, Chae T, and Harlow E (1994). p35 is a neural-specific regulatory subunit of cyclin-dependent kinase 5. *Nature* **371**(6496), 419–423.

[22] Tang D, Yeung J, Lee KY, Matsushita M, Matsui H, Tomizawa K, Hatase O, and Wang JH (1995). An isoform of the neuronal cyclin-dependent kinase 5 (Cdk5) activator. *J Biol Chem* **270**(45), 26897–26903.

[23] Kwon YT, Gupta A, Zhou Y, Nikolic M, and Tsai LH (2000). Regulation of *N*-cadherin–mediated adhesion by the p35-Cdk5 kinase. *Curr Biol* **10**(7), 363–372.

[24] Li BS, Zhang L, Gu J, Amin ND, and Pant HC (2000). Integrin alpha(1) beta(1)–mediated activation of cyclin-dependent kinase 5 activity is involved in neurite outgrowth and human neurofilament protein H Lys-Ser-Pro tail domain phosphorylation. *J Neurosci* **20**(16), 6055–6062.

[25] Wang CL (2001). Caldesmon and smooth-muscle regulation. *Cell Biochem Biophys* **35**(3), 275–288.

[26] Mirzapoiazova T, Kolosova IA, Romer L, Garcia JG, and Verin AD (2005). The role of caldesmon in the regulation of endothelial cytoskeleton and migration. *J Cell Physiol* **203**(3), 520–528.

[27] Eves R, Webb BA, Zhou S, and Mak AS (2006). Caldesmon is an integral component of podosomes in smooth muscle cells. *J Cell Sci* **119**(Pt 9), 1691–1702.

[28] Morita T, Mayanagi T, Yoshio T, and Sobue K (2007). Changes in the balance between caldesmon regulated by p21-activated kinases and the Arp2/3 complex govern podosome formation. *J Biol Chem* **282**(11), 8454–8463.

[29] Yoshio T, Morita T, Kimura Y, Tsujii M, Hayashi N, and Sobue K (2007). Caldesmon suppresses cancer cell invasion by regulating podosome/invadopodium formation. *FEBS Lett* **581**(20), 3777–3782.

[30] Jain P, Flaherty PT, Yi S, Chopra I, Bleasdell G, Lipay J, Ferandin Y, Meijer L, and Madura JD (2011). Design, synthesis, and testing of a 6-*O*-linked series of benzimidazole based inhibitors of CDK5/p25. *Bioorg Med Chem* **19**(1), 359–373.

[31] Helal CJ, Sanner MA, Cooper CB, Gant T, Adam M, Lucas JC, Kang Z, Kupchinsky S, Ahlijanian MK, and Tate B, et al (2004). Discovery and SAR of 2-aminothiazole inhibitors of cyclin-dependent kinase 5/p25 as a potential treatment for Alzheimer's disease. *Bioorg Med Chem Lett* **14**(22), 5521–5525.

[32] Vulpetti A, Casale E, Roletto F, Amici R, Villa M, and Pevarello P (2006). Structure-based drug design to the discovery of new 2-aminothiazole CDK2 inhibitors. *J Mol Graph Model* **24**(5), 341–348.

[33] Lambert de Rouvroit C and Goffinet AM (2001). Neuronal migration. *Mech Dev* **105**(1-2), 47–56.

[34] Ohshima T, Ward JM, Huh CG, Longenecker G, Veeranna, Pant HC, Brady RO, Martin LJ, and Kulkarni AB (1996). Targeted disruption of the cyclin-dependent kinase 5 gene results in abnormal corticogenesis, neuronal pathology and perinatal death. *Proc Natl Acad Sci U S A* **93**(20), 11173–11178.

[35] Schutte U, Bisht S, Brossart P, and Feldmann G (2011). Recent developments of transgenic and xenograft mouse models of pancreatic cancer for translational research. *Expert Opin Drug Discov* **6**(1), 33–48.

[36] Jin JK, Tien PC, Cheng CJ, Song JH, Huang C, Lin SH, and Gallick GE (2014). Talin1 phosphorylation activates beta1 integrins: a novel mechanism to promote prostate cancer bone metastasis. *Oncogene* **34**, 1811–1821

[37] Eggers JP, Grandgenett PM, Collisson EC, Lewallen ME, Tremayne J, Singh PK, Swanson BJ, Andersen JM, Caffrey TC, and High RR, et al (2011). Cyclin-dependent kinase 5 is amplified and overexpressed in pancreatic cancer and activated by mutant K-Ras. *Clin Cancer Res* **17**(19), 6140–6150.

[38] Hu C, Dadon T, Chenna V, Yabuuchi S, Bannerji R, Booher R, Strack P, Azad N, Nelkin BD, and Maitra A (2015). Combined inhibition of cyclin-dependent kinases (dinaciclib) and AKT (MK-2206) blocks pancreatic tumor growth and metastases in patient-derived xenograft models. *Mol Cancer Ther* **14**, 1532–1539

[39] Ehrlich SM, Liebl J, Ardelt MA, Lehr T, De Toni EN, Mayr D, Brandl L, Kirchner T, Zahler S, and Gerbes AL, et al (2015). Targeting cyclin dependent kinase 5 in hepatocellular carcinoma—a novel therapeutic approach. *J Hepatol* **63**, 102–113

[40] Zhong B, Wang T, Lun X, Zhang J, Zheng S, Yang W, Li W, Xiang AP, and Chen Z (2014). Contribution of nestin positive esophageal squamous cancer cells on malignant proliferation, apoptosis, and poor prognosis. *Cancer Cell Int* **14**, 57.

[41] Lin H, Chen MC, Chiu CY, Song YM, and Lin SY (2007). Cdk5 regulates STAT3 activation and cell proliferation in medullary thyroid carcinoma cells. *J Biol Chem* **282**(5), 2776–2784.

[42] Pozo K, Castro-Rivera E, Tan C, Plattner F, Schwach G, Siegl V, Meyer D, Guo A, Gundara J, and Mettlach G, et al (2013). The role of Cdk5 in neuroendocrine thyroid cancer. *Cancer Cell* **24**(4), 499–511.

[43] Pozo K, Hillmann A, Augustyn A, Plattner F, Hai T, Singh T, Ramezani S, Sun X, Pfragner R, and Minna JD, et al (2015). Differential expression of cell cycle regulators in CDK5-dependent medullary thyroid carcinoma tumorigenesis. *Oncotarget* **6**, 12080–12093

[44] Levacque Z, Rosales JL, and Lee KY (2012). Level of cdk5 expression predicts the survival of relapsed multiple myeloma patients. *Cell Cycle* **11**(21), 4093–4095.

[45] Kumar SK, LaPlant B, Chng WJ, Zonder J, Callander N, Fonseca R, Fruth B, Roy V, Erlichman C, and Stewart AK, et al (2014). Dinaciclib, a novel CDK inhibitor, demonstrates encouraging single agent activity in patients with relapsed multiple myeloma. *Blood* **125**, 443–448

[46] Lowman XH, McDonnell MA, Kosloske A, Odumade OA, Jenness C, Karim CB, Jemmerson R, and Kelekar A (2010). The proapoptotic function of Noxa in human leukemia cells is regulated by the kinase Cdk5 and by glucose. *Mol Cell* **40**(5), 823–833.

[47] Tripathi BK, Qian X, Mertins P, Wang D, Papageorge AG, Carr SA, and Lowy DR (2014). CDK5 is a major regulator of the tumor suppressor DLC1. *J Cell Biol* **207**(5), 627–642.

[48] Leshchenko VV, Kuo PY, Shaknovich R, Yang DT, Gellen T, Petrich A, Yu Y, Remache Y, Weniger MA, and Rafiq S, et al (2010). Genomewide DNA methylation analysis reveals novel targets for drug development in mantle cell lymphoma. *Blood* **116**(7), 1025–1034.

[49] Liebl J, Weitensteiner SB, Vereb G, Takacs L, Furst R, Vollmar AM, and Zahler S (2010). Cyclin-dependent kinase 5 regulates endothelial cell migration and angiogenesis. *J Biol Chem* **285**(46), 35932–35943.

[50] Weitensteiner SB, Liebl J, Krystof V, Havlicek L, Gucky T, Strnad M, Furst R, Vollmar AM, and Zahler S (2013). Trisubstituted pyrazolopyrimidines as novel angiogenesis inhibitors. *PLoS One* **8**(1), e54607.

[51] Quintavalle M, Elia L, Price JH, Heynen-Genel S, and Courtneidge SA (2011). A cell-based high-content screening assay reveals activators and inhibitors of cancer cell invasion. *Sci Signal* **4**(183), ra49.

[52] Matsumura F and Yamashiro S (1993). Caldesmon. *Curr Opin Cell Biol* **5**(1), 70–76.

[53] Yamashiro S, Yoshida K, Yamakita Y, and Matsumura F (1994). Caldesmon: possible functions in microfilament reorganization during mitosis and cell transformation. *Adv Exp Med Biol* **358**, 113–122.

[54] McManus MJ, Boerner JL, Danielsen AJ, Wang Z, Matsumura F, and Maihle NJ (2000). An oncogenic epidermal growth factor receptor signals via a p21-activated kinase-caldesmon-myosin phosphotyrosine complex. *J Biol Chem* **275**(45), 35328–35334.

[55] Boerner JL, Danielsen A, McManus MJ, and Maihle NJ (2001). Activation of Rho is required for ligand-independent oncogenic signaling by a mutant epidermal growth factor receptor. *J Biol Chem* **276**(5), 3691–3695.

[56] Boerner JL, Danielsen AJ, Lovejoy CA, Wang Z, Juneja SC, Faupel-Badger JM, Darce JR, and Maihle NJ (2003). Grb2 regulation of the actin-based cytoskeleton is required for ligand-independent EGF receptor-mediated oncogenesis. *Oncogene* **22**(43), 6679–6689.

[57] Putey A, Fournet G, Lozach O, Perrin L, Meijer L, and Joseph B (2014). Synthesis and biological evaluation of tetrahydro[1,4]diazepino[1,2-a]indol-1-ones as cyclin-dependent kinase inhibitors. *Eur J Med Chem* **83**, 617–629.

[58] Tell V, Holzer M, Herrmann L, Mahmoud KA, Schachtele C, Totzke F, and Hilgeroth A (2012). Multitargeted drug development: Discovery and profiling of dihydroxy substituted 1-aza-9-oxafluorenes as lead compounds targeting Alzheimer disease relevant kinases. *Bioorg Med Chem Lett* **22**(22), 6914–6918.